ADVANCED OPTICAL MATERIALS
www.advopticalmat.de

Ultra-Stretchable Multicolor Fluorescent Hydrogels Based on Polymer Networks Involving both Strong and Weak Crosslinks

Wanning Li, Hao Zhang, Wei Lu, Yi Zhang, Tianjiang Zheng,* Guilin Yang, and Tao Chen**

Owing to their inherent soft wet nature and the capacity to offer tunable emission color/intensity responses, multicolor fluorescent polymeric hydrogels (MFPHs) are attracting tremendous research interests. However, most of the reported MFPHs suffer from poor stretchability, thus restricting their versatile uses in artificial muscles, soft robotics, and so on. In this study, a robust type of lanthanide coordinated MFPHs with an ultra-stretchability of over 1200% is designed and prepared. It is found that the ultra-stretchability originates from the unique polymer network structure, in which a small quantity of strong crosslinking interactions (polymer chain entanglement/fixation around the nano-clay and lanthanide coordination) are utilized to ensure the polymer network integrity, and a large quantity of hierarchical (single, double, and quadruple) hydrogen-bonding interactions are designed to efficiently dissipate energy. Furthermore, a braiding strategy is proposed to tightly twist several hydrogel stripes into mechanical strong hydrogel ropes that still keep the ultra-stretchability (>1000%) but can lift heavy weights >350 times their own weight. This study provides new insights into the design of ultra-stretchable fluorescent hydrogels, and is expected to inspire the future development of multifunctional artificial hydrogel muscles.

1. Introduction

Multicolor fluorescent polymeric hydrogels (MFPHs) have attracted intense research attention due to their promising capacity to enable responsive changes of both emission color and intensity.[1–8] The past decade has witnessed a number of elegant MFPH examples, which were usually synthesized by physically doping or chemically grafting two or more responsive luminogens (e.g., lanthanide complexes,[9–15] organic fluorophores,[16–24] and luminescent nanoparticles[25–31]) into the hydrophilic polymer network. However, most reported fluorescent polymeric hydrogels were usually unstretchable, thus restricting their versatile applications. In this context, several impressive advances have been achieved very recently. For example, Tang, Li et al.[32] recently reported a nanocomposite MFPH system with maximum stretching ratio of ≈700% by introducing pH-responsive tetraphenyl ethylene derivatives into Laponite-toughened cross-linked polyacrylamide networks. Li et al.[33] physically incorporated luminescent molecules into supramolecular poly(*N*-acryloyl glycinamide) (PNAGA) hydrogel to obtain a robust MFPH example, which was capable of utilizing the high-density hydrogen bonds between PNAGA polymer chains to efficiently dissipate energy and thus significantly enhance stretchability (up to ≈700%). Nevertheless, despite these progresses, the construction of ultra-stretchable MFPH system with a stretching ratio beyond 1200% remains a great challenge.

To significantly increase stretchability of MFPH systems, it may be promising to design and synthesize the multiply crosslinked supramolecular polymer network containing both strong and weak crosslinking interactions.[34–45] In such design, it is possible to utilize the weak crosslinking interactions to efficiently dissipate energy, while the strong crosslinking interactions are employed to let them recover as far as possible to the initial length. Herein, we try to demonstrate one such ultra-stretchable MFPH system. Its key design is the synthesis of a new potassium 6-(3-(2-(methacryloyloxy)ethyl)ureido)picolinate (K6MUPA) monomer, which can not only coordinate with Eu^{3+} and Tb^{3+} ions to sensitize their red and green emission via resonance energy transfer,[46] but also form complementary quadruple hydrogen bonds between two K6MUPA dimers.[47] The designed MFPH was then prepared through radical copolymerization of acrylamide (AAm) and K6MUPA monomer in aqueous suspension of nano-clay, followed by the coordination with Eu^{3+} and Tb^{3+} to form red and green fluorescent Eu-K6MUPA and Tb-K6MUPA complexes. **Scheme 1** illustrates the polymer network structure of this MFPH system, in which

W. Li, W. Lu, Y. Zhang, T. Chen
Key Laboratory of Marine Materials and Related Technologies
Zhejiang Key Laboratory of Marine Materials and Protective Technologies
Ningbo Institute of Materials Technology and Engineering
Chinese Academy of Sciences
Ningbo 315201, P. R. China
E-mail: luwei@nimte.ac.cn; tao.chen@nimte.ac.cn
W. Li, H. Zhang, W. Lu, T. Zheng, G. Yang, T. Chen
School of Chemical Sciences
University of Chinese Academy of Sciences
E-mail: 19A Yuquan Road, Beijing 100049, P. R. China;
zhengtianjiang@nimte.ac.cn
H. Zhang, T. Zheng, G. Yang
Zhejiang Key Laboratory of Robotics and Intelligent Manufacturing Equipment Technology
Ningbo Institute of Materials Technology and Engineering
Chinese Academy of Sciences
Ningbo 315201, P. R. China
The ORCID identification number(s) for the author(s) of this article can be found under https://doi.org/10.1002/adom.202202738.

DOI: 10.1002/adom.202202738

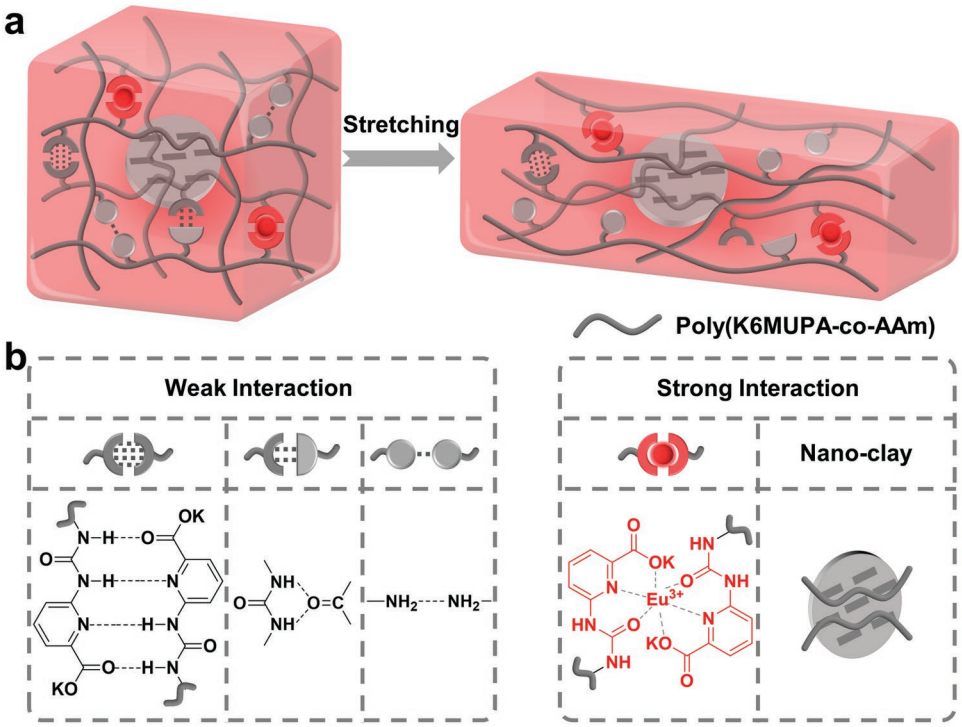

Scheme 1. a) Illustrated polymer network design of the ultra-stretchable MFPH system and b) chemical structures of the involved strong and weak crosslinks.

a small quantity of strong crosslinking interactions (polymer chain entanglement/fixation around the nano-clay and lanthanide coordination) were utilized to ensure the polymer network integrity, and a large quantity of hierarchical (single, double, and quadruple) hydrogen-bonding interactions were designed to efficiently dissipate energy. As a result, ultra-stretchable MFPHs with the stretching ratio beyond 1200% were obtained. To further increase its toughness, a braided strategy was proposed to twist several ultra-stretchable thin hydrogel stripes into the braided hydrogel ropes that could sustain more than 350 times their body weight, suggesting their potential use for high-strength artificial muscles.[48]

2. Results and Discussion

The key step in preparing supramolecular multicolor fluorescent hydrogels is the design and synthesis of the specific ligand monomer, 6MUPA that contains the urea and picolinic acid group. **Figure 1**a illustrates its synthetic procedure by an addition reaction between the amino group of 6-aminopyridine-2-carboxylic acid and the isocyanate group of 2-isocyanatoethyl methacrylate at room temperature (Figure S1, Supporting Information). This specially designed new monomer was clearly characterized by ^{1}H NMR, ^{13}C NMR, and ESI-MS spectroscopies. As shown in Figure 1b,c, the typical ^{1}H signal around 13.2 ppm (COOH hydrogen) and multiple peaks at 7–8 ppm (pyridine hydrogen) as well as the ^{13}C signal at 166.8 ppm (COOH group) clearly indicated the introduction of picolinic acid moieties into the 6MUPA monomer. The chemical structure was further verified by Fourier Transform Infrared (FT-IR) spectroscopies (Figure S2, Supporting Information). Figure 1d reveals the molecular weight of 6MUPA to be 294.1 ([M + H]$^{+}$), which is also consistent with the designed molecule. With long hydrophobic units, 6MUPA is readily soluble in DMSO and DMF, but nearly insoluble in deionized water. In order to facilitate its introduction into the polymeric hydrogel matrix, its water-soluble potassium salt (K6MUPA) was prepared by reacting 6MUPA with equimolar amount of KOH. Aqueous solution of K6MUPA had a broad absorption peak about 300 nm (Figure S3, Supporting Information) and was non-fluorescent under 254 nm UV light.

Figure 2a illustrates the synthetic procedure of supramolecular poly(K6MUPA-*co*-AAm) hydrogels by heat-initiated radical copolymerization of acrylamide (AAm) and K6MUPA monomer in aqueous suspension of nano-clay (Figure S4, Supporting Information). The molar feed ratio of K6MUPA/AAm was set as 1/49 and the polymerization was carried out at 60 °C for 8 h. In this polymerization process, entanglement and fixation of polymer chains were induced around the clay nanosheets. Meanwhile, hierarchical (single, double, and quadruple) hydrogen-bonding interactions between the grafted ureido-picolinate moieties and primary amide groups were formed to induce hydrogen bonded (H-bonded) polymer network, as evidenced by the FT-IR spectra shown in Figure 2b–d. Upon raising temperature from 30 to 100 °C, intensity of the broad peaks around 3400 cm^{-1} (H-bonded N—H) and 1675 cm^{-1} (H-bonded C = O) gradually decreased accompanying with enhanced intensity of the shoulder peak around 3600 cm^{-1} (free N—H) and 1750 cm^{-1} (free C = O). 2D correlation spectra were further conducted (Figure 2e,f), which suggested the H-bonded groups have weaker motility

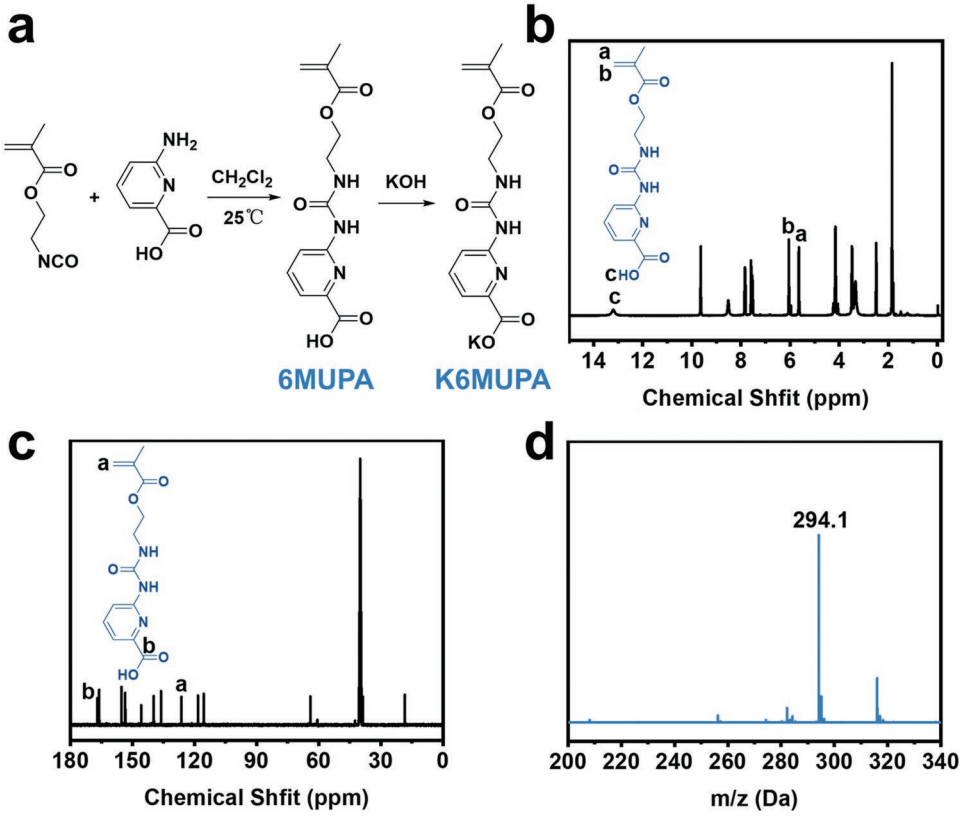

Figure 1. a) Synthetic procedure of the ligand monomer 6MUPA and K6MUPA. b) ^{1}H and c) ^{13}C NMR spectra of 6MUPA in DMSO-d_6. d) ESI-MS result of 6MUPA.

and higher sensitivity to temperature than free groups, as reflected by the observation that the auto peaks in the synchronous spectra at (1675, 1675 cm^{-1}) and (3400, 3400 cm^{-1}) are more obvious than those in the (1750, 1750 cm^{-1}) and (3600, 3600 cm^{-1}) region.[49] All these results demonstrated there are plenty of hierarchical (single, double, and quadruple) hydrogen-bonds in the obtained poly(K6MUPA-*co*-AAm) hydrogel.

To realize multicolor fluorescence, Eu^{3+} and Tb^{3+} were then employed to coordinate with the grafted K6MUPA moieties to produce Eu/Tb-poly(K6MUPA-*co*-AAm) with red and green fluorescent Eu-K6MUPA and Tb-K6MUPA centers (**Figure 3**a). Figures S5–S7, Supporting Information, compares their fluorescence spectra and UV–vis spectra. It was found that the K6MUPA monomer and poly(K6MUPA-*co*-AAm) hydrogel were nearly non-fluorescent under the excitation of 254 nm UV light. But upon coordination with lanthanide ions, the as-prepared Eu-poly(K6MUPA-*co*-AAm) and Tb-poly(K6MUPA-*co*-AAm) hydrogels turned to emit intense red and green fluorescence, respectively.[50] In particular, the transparent poly (K6MUPA-*co*-AAm) hydrogel transformed into a white opaque state after the introduction of Eu^{3+} and Tb^{3+} (Figures S8 and S9, Supporting Information), and SEM images showed tighter porous structure (Figure S10, Supporting Information), which further demonstrated the formation of additional metal coordination. Furthermore, multicolor fluorescent Eu/Tb-poly(K6MUPA-*co*-AAm) hydrogels were prepared by immersing the poly(K6MUPA-*co*-AAm) hydrogels into mixed Eu^{3+}/Tb^{3+} solutions to induce the formation of red and green fluorescent centers (Figure S11, Supporting Information). As shown in Figure 3b, the red emission peak at about 615 nm gradually increased at the cost of the green emission band around 545 nm upon varying the Eu^{3+}/Tb^{3+} molar ratio. Correspondingly, emission color of the hydrogels was facilely adjusted from red to yellow and then green (Figure 3c,d), indicating the wide emission color tunability of the obtained Eu/Tb-poly(K6MUPA-*co*-AAm) hydrogels.

Mechanical properties of the obtained supramolecular multicolor fluorescent Eu/Tb-poly(K6MUPA-*co*-AAm) hydrogels were then studied. As detailed above, the as-prepared Eu/Tb-poly(K6MUPA-*co*-AAm) hydrogels have multiple supramolecular crosslinks. There are a small quantity of strong polymer chain entanglement around the nano-clay and lanthanide coordination interactions, as well as a large quantity of weak hierarchical hydrogen-bonding interactions, including quadruple ones between K6MUPA dimers, double ones between $-NH_2$ and C = O groups, as well as the single ones between two $-NH_2$ groups. As a result, the Eu/Tb-poly(K6MUPA-*co*-AAm) hydrogel stripes were proved to have extremely good stretchability. As can be seen from **Figure 4**a, one Eu/Tb-poly(K6MUPA-*co*-AAm) hydrogel strip (10 mm × 2 mm × 1.8 mm, 80 wt% water content) could be stretched up to 450% and fully restored to its initial length within 2 s. Tensile experiments demonstrated that it could sustain a fracture stress of 427.1 kPa and extremely large tensile strain over 1200% (Figure 4b). When the hydrogel was tested for tensile loading–unloading without interval, a significant hysteresis phenomenon was observed

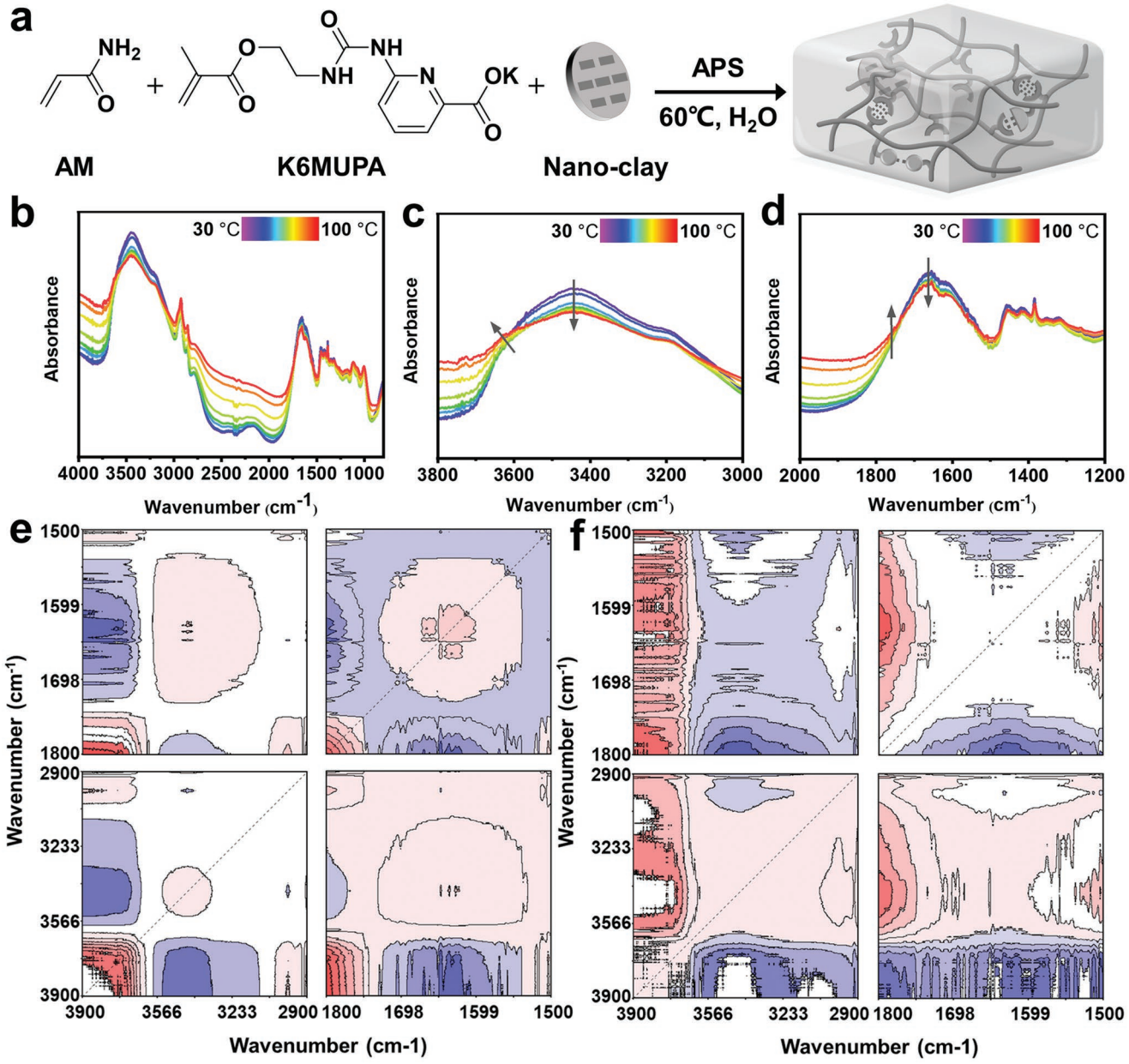

Figure 2. a) Schematic illustration showing the synthetic procedure of supramolecular poly(K6MUPA-*co*-AAm) hydrogel. Temperature-dependent FT-IR spectra of the freeze-dried poly(K6MUPA-*co*-AAm) hydrogel at b) 4000–800 cm^{-1}, c) 3800–3000 cm^{-1}, d) 2000–1200 cm^{-1}. e) Synchronous and f) asynchronous generalized 2D correlation spectra of the correlation of hydrogen bond. Synchronous and asynchronous 2D correlation spectra, in which red and blue colors represent positive and negative intensity, respectively.

as the strain increased from 50% to 500% (Figure 4c), indicating the existence of an effective energy dissipation process in the Eu/Tb-poly(K6MUPA-*co*-AAm) hydrogel. Furthermore, mechanical properties of the hydrogel were not significantly changed after 10 consecutive cycles of loading at 200% strain (Figure 4d), proving that the broken weak hydrogen-bonded crosslinking interactions in the former cycle could be rapidly restored in the subsequent cycle. Owing to such good stretchability, the Eu-poly(K6MUPA-*co*-AAm) and Tb-poly(K6MUPA-*co*-AAm) hydrogel stripes could be easily bent, twisted, and knotted (Figure 4e). Besides, the capacity to offer electrostatic interactions of nano-clay and high-density supramolecular hydrogen bonds also endowed the hydrogel with good adhesion to skin, metal, glass, plastic, rubber, PDMS, PP, carton, and leaf (Figure 4f and Figure S12, Supporting Information), suggesting its multi-functional potential.

Human muscles are strong and durable because of their multistage structure, which evenly distributes stress and effectively dissipates energy.[51–54] Inspired by this finding, one braiding strategy was proposed to transform the ultra-stretchable Eu-poly(K6MUPA-*co*-AAm) into braided hydrogel ropes by twist insertion. To this end, thin hydrogel stripes, having a dimension

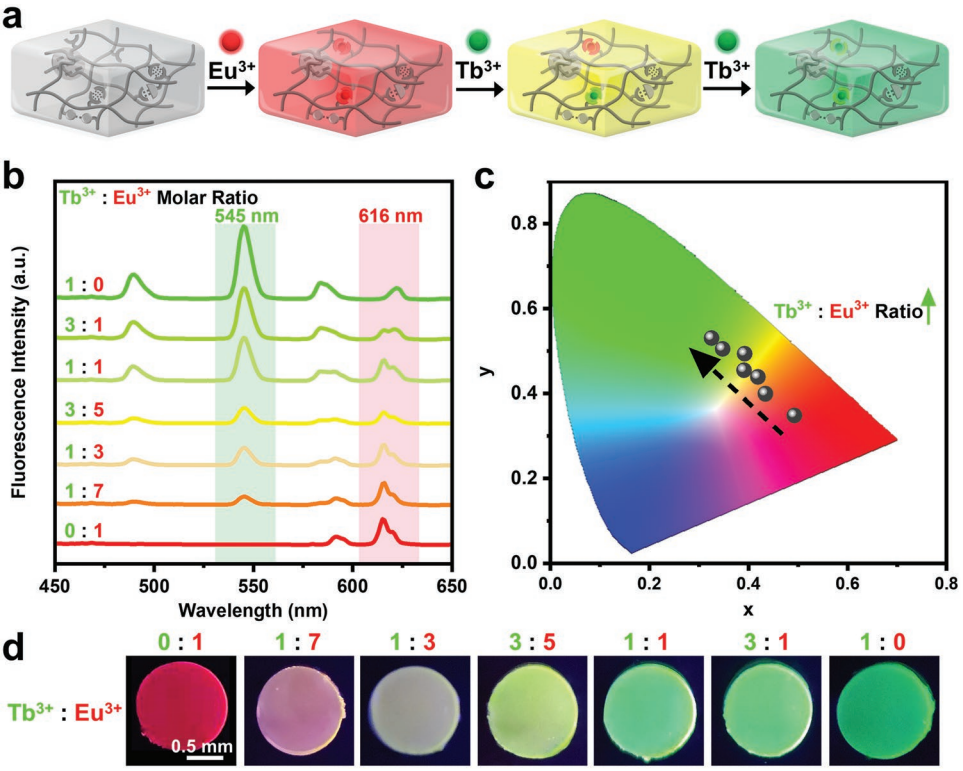

Figure 3. a) Scheme of the multicolor fluorescent Eu/Tb-poly(K6MUPA-*co*-AAm) hydrogels containing red and green fluorescent Eu-K6MUPA and Tb-K6MUPA centers. b) Fluorescence spectra (λ_{ex} = 254 nm) of Eu/Tb-poly(K6MUPA-*co*-AAm) hydrogels with different Tb/Eu ratios and c) their corresponding coordinates in the CIE (1931) coordinate diagram, as well as d) fluorescent photos taken under a 254 nm UV lamp.

of 80 mm × 2 mm × 1.8 mm (length × width × thickness), were cut from one bulk Eu-poly(K6MUPA-*co*-AAm) hydrogel with a solid content of 20 wt% by using a laser cutter. Next, these hydrogel strips were twisted through a twisting device (Figure S13, Supporting Information) and folded in half by hands. Finally, these two halves could self-twist into one hydrogel rope with stable double-helix structure for the purpose of achieving force equilibrium (**Figure 5**a). In this braided

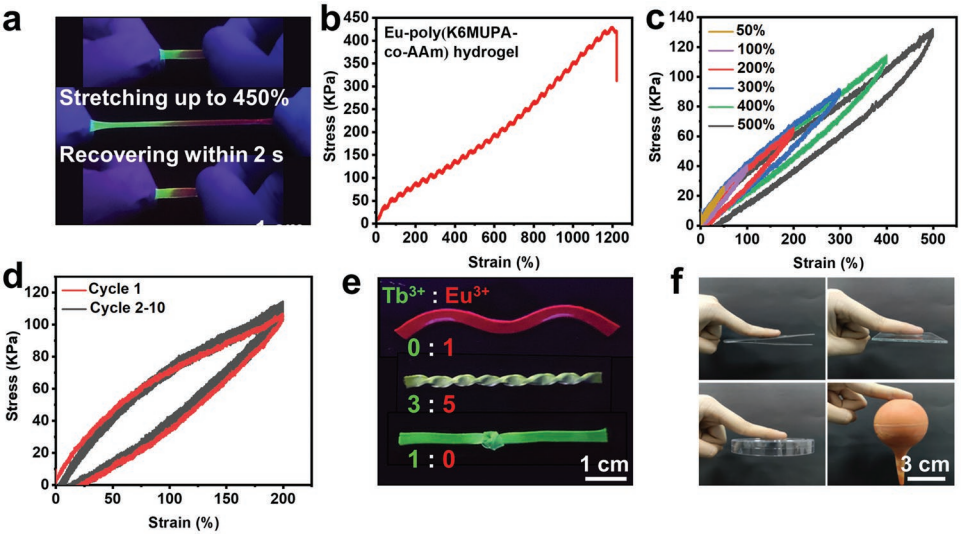

Figure 4. a) Photos showing the ultra-stretching and fast recovery processes of the Eu/Tb-poly(K6MUPA-*co*-AAm) hydrogel with 80 wt% water content, which were taken under a 254 nm UV lamp. b) Tensile stress–strain curve of Eu-poly(K6MUPA-*co*-AAm) hydrogel. c) Tensile loading–unloading curves of Eu-poly(K6MUPA-*co*-AAm) hydrogel at varied strain from 50% to 500%. d) Ten successive loading–unloading cycles of Eu-poly(K6MUPA-*co*-AAm) hydrogel at a strain of 200%. e) Photos showing the capacity of Eu/Tb-poly(K6MUPA-*co*-AAm) hydrogel stripes to enable bending, twisting, and knotting, which were taken under a 254 nm UV lamp. f) Adhesion of Eu-poly(K6MUPA-*co*-AAm) hydrogel to various substrate surfaces at room temperature.

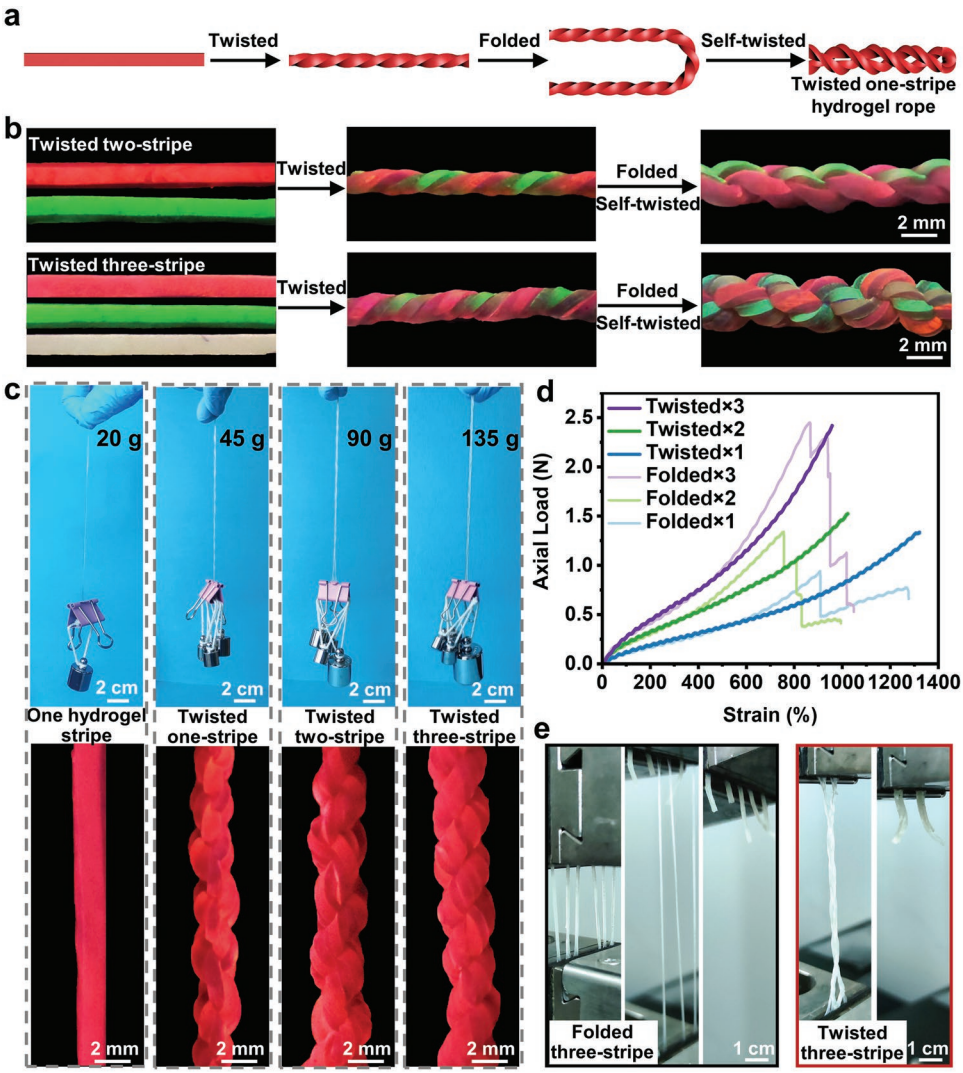

Figure 5. a) Scheme of the preparation process of the twisted one-stripe hydrogel rope. First, the hydrogel strip was twisted through a twisting device. Next, the above strip was folded in half by hand. Finally, the two halves self-twist to achieve force equilibrium. b) Fluorescence photos of multicolor fluorescent hydrogel ropes, red stripe: Eu-poly(K6MUPA-*co*-AAm) hydrogel, green stripe: Tb-poly(K6MUPA-*co*-AAm) hydrogel, yellow stripe: Eu/Tb-poly(K6MUPA-*co*-AAm) hydrogel (Tb^{3+}:Eu^{3+} molar ratio = 3:5). c) Photos showing the tightly twisting structures of the twisted hydrogel ropes prepared by weaving one, two, or three hydrogel stripes and their capacity to lift heavy weights. d) Comparison of the axial load–strain curves of the folded hydrogel stripes and their twisted hydrogel ropes. e) Photos showing the stretching process of the folded three-stripe hydrogel and their twisted hydrogel rope.

structure, both the fracture strength and strain are expected to increase, because the loads borne between the hydrogel stripes were evenly distributed.[55] As shown in Figure 5b,c, uniform twirling hydrogel ropes could be facilely prepared by weaving one, two, or three hydrogel stripes, respectively, according to the above-established method. Especially, different colored fluorescent hydrogel stripes could be braided together for visualizing the texture structure of our hydrogel ropes. Astonishingly, these twisted hydrogel ropes were found to lift ≈350 times as heavy as their own weight, which were significantly higher than the corresponding folded hydrogel stripes (Figures S14 and S15, Supporting Information). As reflected in the axial load–strain curve (Figure 5d), these braided hydrogel ropes also have higher fracture strain. Meanwhile, the ultra-stretchability of Eu-poly(K6MUPA-*co*-AAm) hydrogel was also well-preserved in the twisted hydrogel ropes. The stretchability of twisted one-stripe hydrogel rope still kept above 1200%, and the twisted three-stripe hydrogel rope could also be stretched to about 1000% (Figure S16, Supporting Information). These advantageous properties were believed to come from the following reasons. For those folded hydrogel stripes, the applied stress was usually unevenly distributed on each hydrogel stripe. As a result, the hydrogel stripe that sustain the maximum stress would break first to cause structural failure of the whole system. But things were different for the tightly twisted hydrogel ropes, in which the applied stress was evenly distributed among every hydrogel stripe. As demonstrated in Figure 5e, they broke only when the applied stress is large enough to simultaneously break all hydrogel stripes. All these results clearly demonstrated robust potential of the proposed braided strategy to

simultaneously enhance the fracture strength and load-bearing capacity of polymeric hydrogels without significantly affecting their ultra-stretchability.

3. Conclusion

We have constructed a robust kind of lanthanide coordinated MFPHs with ultra-stretchability of above 1200%. Its core design is the synthesis of a multifunctional K6MUPA monomer, which is not only able to sensitize the Eu^{3+} and Tb^{3+} luminescence to produce red and green fluorescent lanthanide complexes, but also form quadruple hydrogen bonds between two K6MUPA dimers. Its chemical introduction into supramolecular nanoclay-containing poly(K6MUPA-*co*-AAm) hydrogel matrix spontaneously produces tunable multicolor fluorescence depending on the Eu^{3+}/Tb^{3+} doping ratio. Importantly, such molecular design results in the unique polymer network, which includes a large number of hierarchical (single, double, and quadruple) hydrogen bonds that can efficiently dissipate energy during the stretching process, and a small number of strong crosslinking interactions (polymer chain entanglement/fixation around the nano-clay and lanthanide coordination) that can ensure the polymer network integrity. Consequently, the developed multicolor fluorescent Eu/Tb-poly(K6MUPA-*co*-AAm) hydrogels are capable of sustaining an extremely high stretching ratio beyond 1200%. Finally, a braided strategy was proposed to tightly twist several ultra-stretchable hydrogel stripes into strong braided hydrogel ropes that could lift heavy weights >350 times their own weight without significantly affecting their ultra-stretchability. The proposed design of cross-linked polymer network is believed to generally applicable to produce many different types of ultra-stretchable multicolor fluorescent hydrogel systems. Together with the developed hydrogel braiding strategy, ultra-stretchable MFPHs with high stress will be envisaged in the near future, which are expected to find wide uses in artificial muscles, soft actuators/robotics, and so on.

Supporting Information

Supporting Information is available from the Wiley Online Library or from the author.

Acknowledgements

W.L. and H.Z. contributed equally to this work. This work was supported by the Zhejiang Provincial Natural Science Foundation of China (LD22E050008), the Sino-German Mobility Programme (M-0424), the Youth Innovation Promotion Association of Chinese Academy of Sciences (2019297), the K. C. Wong Education Foundation (GJTD-2019-13), and the National Natural Science Foundation of China (U1909215).

Conflict of Interest

The authors declare no conflict of interest.

Data Availability Statement

The data that support the findings of this study are available from the corresponding author upon reasonable request.

Keywords

braiding, hydrogels, multicolor fluorescence, stretchability

Received: November 17, 2022
Revised: December 25, 2022
Published online: February 12, 2023

[1] Z. Li, X. Ji, H. Xie, B. Z. Tang, *Adv. Mater.* **2021**, *33*, 2100021.
[2] Y. Li, D. J. Young, X. J. Loh, *Mater. Chem. Front.* **2019**, *3*, 1489.
[3] H. Wang, X. Ji, Z. Li, F. Huang, *Adv. Mater.* **2017**, *29*, 1606117.
[4] B. Li, T. He, X. Shen, D. Tang, S. Yin, *Polym. Chem.* **2019**, *10*, 796.
[5] W. Lu, M. Si, X. Le, T. Chen, *Acc. Chem. Res.* **2022**, *55*, 2291.
[6] D. Li, J. Wang, X. Ma, *Adv. Opt. Mater.* **2018**, *6*, 1800273.
[7] H. Xie, Z. Li, J. Gong, L. Hu, P. Alam, X. Ji, Y. Hu, J. H. C. Chau, J. W. Y. Lam, R. T. K. Kwok, B. Tang, *Adv. Mater.* **2021**, *33*, 2105113.
[8] H. Xie, J. Zhang, R. T. K. Kwok, J. W. Y. Lam, Z. Li, B. Tang, *APL Mater.* **2022**, *10*, 080905.
[9] G. Weng, S. Thanneeru, J. He, *Adv. Mater.* **2018**, *30*, 1706526.
[10] X. Xu, J. Wang, B. Yan, *Adv. Funct. Mater.* **2021**, *31*, 2103321.
[11] Q.-F. Li, X. Du, L. Jin, M. Hou, Z. Wang, J. Hao, *J. Mater. Chem. C* **2016**, *4*, 3195.
[12] S. Wei, H. Qiu, H. Shi, W. Lu, H. Liu, H. Yan, D. Zhang, J. Zhang, P. Theato, Y. Wei, T. Chen, *ACS Nano* **2021**, *15*, 10415.
[13] Z. Li, G. Wang, Y. Wang, H. Li, *Angew. Chem., Int. Ed.* **2018**, *57*, 2194.
[14] K. Meng, C. Yao, Q. Ma, Z. Xue, Y. Du, W. Liu, D. Yang, *Adv. Sci.* **2019**, *6*, 1802112.
[15] P. Chen, Q. Li, S. Grindy, N. Holten-Andersen, *J. Am. Chem. Soc.* **2015**, *137*, 11590.
[16] Y. Yang, Q. Li, H. Zhang, H. Liu, X. Ji, B. Z. Tang, *Adv. Mater.* **2021**, *33*, 2105418.
[17] C. N. Zhu, T. Bai, H. Wang, J. Ling, F. Huang, W. Hong, Q. Zheng, Z. L. Wu, *Adv. Mater.* **2021**, *33*, 2102023.
[18] Y. Lin, C. Li, G. Song, C. He, Y. Q. Dong, H. Wang, *J. Mater. Chem. C* **2015**, *3*, 2677.
[19] Z. Wang, J. Nie, W. Qin, Q. Hu, B. Z. Tang, *Nat. Commun.* **2016**, *7*, 12033.
[20] H. Chen, F. Yang, Q. Chen, J. Zheng, *Adv. Mater.* **2017**, *29*, 1606900.
[21] G. Liu, Y.-M. Zhang, X. Xu, L. Zhang, Y. Liu, *Adv. Opt. Mater.* **2017**, *5*, 1700149.
[22] D. Lu, M. Zhu, S. Wu, Q. Lian, W. Wang, D. Adlam, J. A. Hoyland, B. R. Saunders, *Adv. Funct. Mater.* **2020**, *30*, 1909359.
[23] J. Wang, F. Tang, Y. Wang, S. Liu, L. Li, *Adv. Opt. Mater.* **2020**, *8*, 1901571.
[24] X. Ji, Z. Li, Y. Hu, H. Xie, W. Wu, F. Song, H. Liu, J. Wang, M. Jiang, J. W. Y. Lam, B. Tang, *CCS Chem.* **2021**, *3*, 1146.
[25] Y. Yu, Y. Feng, F. Liu, H. Wang, H. Yu, K. Dai, G. Zheng, W. Feng, *Small* **2022**, *18*, 2204365.
[26] S. Bhattacharya, R. S. Phatake, S. N. Barnea, N. Zerby, J. J. Zhu, R. Shikler, N. G. Lemcoff, R. Jelinek, *ACS Nano* **2019**, *13*, 7396.
[27] T. H. Le, Y. Choi, S. Kim, U. Lee, E. Heo, H. Lee, S. Chae, W. B. Im, H. Yoon, *Adv. Opt. Mater.* **2020**, *8*, 1901972.
[28] H. Zhi, X. Fei, J. Tian, M. Jing, L. Xu, X. Wang, D. Liu, Y. Wang, J. Liu, *J. Mater. Chem. B* **2017**, *5*, 5738.
[29] J. Zhang, J. Jin, J. Wan, S. Jiang, Y. Wu, W. Wang, X. Gong, H. Wang, *Chem. Eng. J.* **2021**, *408*, 127351.

[30] X. Y. Du, C. F. Wang, G. Wu, S. Chen, *Angew. Chem., Int. Ed.* **2021**, *60*, 8585.
[31] J. Hai, T. Li, J. Su, W. Liu, Y. Ju, B. Wang, Y. Hou, *Angew. Chem., Int. Ed.* **2018**, *57*, 6786.
[32] G. Su, Z. Li, J. Gong, R. Zhang, R. Dai, Y. Deng, B. Z. Tang, *Adv. Mater.* **2022**, *34*, 2207212.
[33] Q. Zhang, X. Wang, Y. Cong, Y. Kang, Z. Wu, L. Li, *ACS Appl. Mater. Interfaces* **2022**, *14*, 12674.
[34] J. P. Gong, Y. Katsuyama, T. Kurokawa, Y. Osada, *Adv. Mater.* **2003**, *15*, 1155.
[35] Y. Zheng, H. Huang, J. Yu, Z. Hu, Y. Wang, *Chem. Eng. J.* **2023**, *454*, 140054.
[36] M. Zhang, J. Yu, K. Shen, R. Wang, J. Du, X. Zhao, Y. Yang, K. Xu, Q. Zhang, Y. Zhang, Y. Cheng, *Chem. Mater.* **2021**, *33*, 6453.
[37] J. Sautaux, F. Marx, I. Gunkel, C. Weder, S. Schrettl, *Nat. Commun.* **2022**, *13*, 356.
[38] X. Dai, Y. Zhang, L. Gao, T. Bai, W. Wang, Y. Cui, W. Liu, *Adv. Mater.* **2015**, *27*, 3566.
[39] T. Long, Y. Li, X. Fang, J. Sun, *Adv. Funct. Mater.* **2018**, *28*, 1804416.
[40] H. Lei, L. Dong, Y. Li, J. Zhang, H. Chen, J. Wu, Y. Zhang, Q. Fan, B. Xue, M. Qin, B. Chen, Y. Cao, W. Wang, *Nat. Commun.* **2020**, *11*, 4032.
[41] L. Shuai, Z. H. Guo, P. Zhang, J. Wan, X. Pu, Z. L. Wang, *Nano Energy* **2020**, *78*, 105389.
[42] H. Zhang, Y. Wu, J. Yang, D. Wang, P. Yu, C. T. Lai, A. C. Shi, J. Wang, S. Cui, J. Xiang, N. Zhao, J. Xu, *Adv. Mater.* **2019**, *31*, 1904029.
[43] L. Voorhaar, R. Hoogenboom, *Chem. Soc. Rev.* **2016**, *45*, 4013.
[44] Z. Li, Z. Lin, *Aggregate* **2021**, *2*, 21.
[45] K. Cui, J. Gong, *Aggregate* **2021**, *2*, 33.
[46] S. Wei, W. Lu, X. Le, C. Ma, H. Lin, B. Wu, J. Zhang, P. Theato, T. Chen, *Angew. Chem., Int. Ed.* **2019**, *58*, 16243.
[47] M. Si, H. Shi, H. Liu, H. Shang, G. Yin, S. Wei, S. Wu, W. Lu, T. Chen, *Mater. Chem. Front.* **2021**, *5*, 5130.
[48] M. Ren, J. Qiao, Y. Wang, K. Wu, L. Dong, X. Shen, H. Zhang, W. Yang, Y. Wu, Z. Yong, W. Chen, Y. Zhang, J. Di, Q. Li, *Small* **2021**, *17*, 2006181.
[49] J. Zhang, W. Wang, Y. Zhang, Q. Wei, F. Han, S. Dong, D. Liu, S. Zhang, *Nat. Commun.* **2022**, *13*, 5214.
[50] Y. Qiao, Y. Lin, S. Zhang, J. Huang, *Chem. - Eur. J.* **2011**, *17*, 5180.
[51] C. S. Haines, M. D. Lima, N. Li, G. M. Spinks, J. Foroughi, J. D. W. Madden, S. H. Kim, S. Fang, M. J. de Andrade, F. Goktepe, O. Goktepe, S. M. Mirvakili, S. Naficy, X. Lepro, J. Oh, M. E. Kozlov, S. J. Kim, X. Xu, B. J. Swedlove, G. G. Wallace, R. H. Baughman, *Science* **2014**, *343*, 868.
[52] Y. Cui, D. Li, C. Gong, C. Chang, *ACS Nano* **2021**, *15*, 13712.
[53] J. Mu, M. J. de Andrade, S. Fang, X. Wang, E. Gao, N. Li, S. H. Kim, H. Wang, C. Hou, Q. Zhang, M. Zhu, D. Qian, H. Lu, D. Kongahage, S. Talebian, J. Foroughi, G. Spinks, H. Kim, T. H. Ware, H. J. Sim, D. Y. Lee, Y. Jang, S. J. Kim, R. H. Baughman, *Science* **2019**, *365*, 150.
[54] A. R. Gillies, R. L. Lieber, *Muscle Nerve* **2011**, *44*, 318.
[55] N. Park, J. Kim, *ACS Appl. Mater. Interfaces* **2022**, *14*, 4479.